Research Article **www.ijcps.com**

International Journal of Chemical and Pharmaceutical Sciences
2018, Jan., Vol. 9 (1)

ISSN: 0976-9390
IJCPS

Inclusion complexation of methyl orange and methyl red with α- and β-cyclodextrin: spectral and theoretical study

Thendral P and Thulasidhasan J*.

Department of Chemistry, School of Arts and Science, Ponnaiyaha Ramajayam Institute of Science and Technology, Thanjavur, Tamilnadu, India.

***Corresponding Author:** E-Mail**:** drthulasi86@gmail.com

Received: 12th Jan 2018, Revised and Accepted: 18th Jan 2018

ABSTRACT

The inclusion complexation behavior of methyl orange (MO) and methyl red (MR) with α-CD and β-CD are examined by absorption, fluorescence, life time and molecular modeling methods. MO and MR form 1:1 (CD/drug) inclusion complexes in lower CD concentrations and 1:2 (CD/drug) inclusion complexes with higher CD concentrations. The inclusion of both dyea with β-CDs was stronger than that of α-CDs. Both dyes exhibit similar emission (excimer) in the CDs solution. The hydrogen bonding and van der Waals interaction between the dyes and the CD plays an important role in the inclusion complexes. Computational results show the dye molecules encapsulated in the CD cavity. The molecular modeling results by PM3 were in good agreement with the experimental results.

Keywords: Methyl orange, methyl red, self assembly, cyclodextrin, molecular modeling.

1. INTRODUCTION

Cyclodextrins (CDs) are a group of cyclic oligosaccharides consisting of 6–8 units of 1, 4-linked glucose units. The spaces of these macromolecules are expressed as circular table shape with different diameters [1]. The property of the inner cavity is hydrophobic, while the outer side is hydrophilic [2]. So the CDs performed as good host for water soluble and fat soluble compounds. The applications of CDs have been extensively investigated to improve the stability and solubility of poor water soluble compounds by formation of inclusion complexes [3–5].

Several works which focused on the reaction between cyclodextrins and volatile oils have been carried out [6–8]. The water-solubility of garlic oil was increased by forming inclusion complex with HP-β-CD [9].

Among the different types of dyes, recently, azo dyes have been used in protein–dye chromatography, which could be important with respect to protein purification [10]. Azo compounds are also used in the pharmaceutical industry. Azo compounds show anti-inflammatory, antimicrobial, or antiparasitic activity, antiulcer drug, antifungal, antibacterial, antitubercular, antibiotics [11, 12].

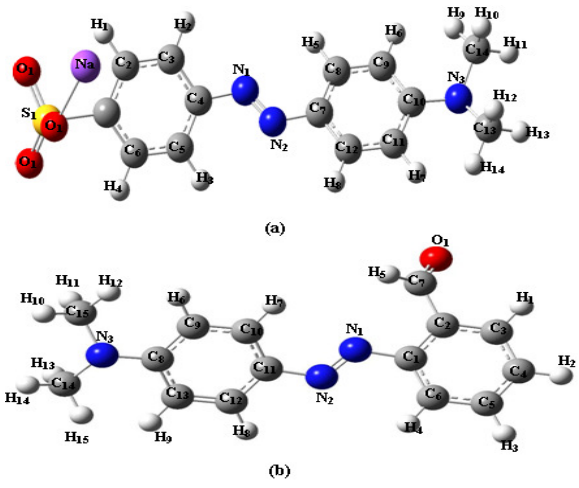

Figure – 1: The optimized structure of (a) Methyl orange and (b) methyl red.

Hence, the analysis of binding of azo dyes with host molecule like cyclodextrin is useful. These azo food dyes are toxic in nature, and hence such explorations can be important from the toxicological point of view.

Here, we focus on the study of the binding effects of two azo dyes namely methyl orange and methyl red (Figure. 1) were investigated by UV-visible, steady state fluorescence spectroscopy,

and the binding process were also performed by using molecular modeling method.

2. EXPERIMENTAL SECTION

2.1. Materials

MO, MR, α-CD and β-CD was purchased from Sigma-Aldrich chemical company and used without further purification. The purity of the compound was checked for similar fluorescence spectra when excited with different wavelengths.

2.2. Preparation of CD Solution

The concentration of stock solution of the dyes were $2x10^{-3}$ M. The stock solution (0.2ml) was transferred into 10ml volumetric flasks. To this, varying concentration of CD solution (1.0×10^{-3} to 1.0×10^{-2} M) was added. The mixed solution was diluted to 10 ml with triply distilled water and shaken thoroughly. The final concentration of dyes in all the flasks was 4×10^{-5} M. The experiments were carried out at room temperature at 300 K.

2.3. Instruments

Absorption spectra were measured with a Shimadzu UV 1601 PC model UV-Visible spectrophotometer. Steady state fluorescence spectra were recorded with a Shimadzu spectrofluorimeter model RF-5301. The pH values in the range 2.5-12.0 were measured on an Elico pH meter (model LI-120).

The fluorescence lifetime measurements were performed using a picoseconds laser and single photon counting setup from Jobin-Vyon IBH. A diode pumped Millena CW laser (Spectra Analysis) 532 nm was used to pump the Ti-Sapphire rod in Tsunami picosecond mode locked laser system (Spectra physics Model No. 4690 M3S). The Ti-Sapphire rod is oriented at Brewster's angle to the laser beam. The wavelength turning range is 720-850 nm, i.e, standard pico configuration. The fluorescence decay of the sample is further analysed using IBH data analysis software. The fluorescence decay profiles were fitted to the expression:

$$I(t) = A_1 \exp\left(\frac{-t}{\tau_1}\right) + A_2 \exp\left(\frac{-t}{\tau_2}\right) \quad (1)$$

$$I(t) = A_1 \exp\left(\frac{-t}{\tau_1}\right) + A_2 \exp\left(\frac{-t}{\tau_2}\right) + A_3 \exp\left(\frac{-t}{\tau_3}\right) \quad (2)$$

where τ_1, τ_2 and τ_3 are lifetimes of the three components, A_1, A_2 and A_3 are the pre-exponential factors of the same and t is time. The average fluorescence lifetime is calculated by using the equation:

$$\langle \tau \rangle = \sum \tau_i a_i \quad (3)$$

2.4. Molecular Modeling Studies

The theoretical calculations were performed with Gaussian 03W package. The initial geometry of the SMP, α-CD and β-CD was constructed with the aid of Spartan 08 and then optimized by the semiempirical PM3 method at vacuum. The CD was fully optimized by PM3 without any symmetry constraint [13]. The glycosidic oxygen atoms of CD were placed onto the XY plane and their center was defined as the center of the coordinate system. The primary hydroxyl groups were placed pointing toward the positive Z axis. The inclusion complex was constructed from the PM3 optimized CD and guest molecules. The longest dimension of the guest molecule was initially placed onto the Z axis. The position of the guest was determined by the Z coordinate of one selected atom of the guest. The inclusion process was simulated by putting the guest on one end of the CD and then letting it pass through the CD cavities. Since the semiempirical PM3 method has been proved to be a powerful tool in the conformational study of CD inclusion complexes and has high computational efficiency [14], we selected semiempirical PM3 method to study the inclusion process of CDs with the dye molecules.

3. RESULTS AND DISCUSSION

3.1. Effect of cyclodextrins with MO and MR

Figures.2 and 3, depict the absorption and emission spectra of MO and MR (2×10^{-5} M) in pH ~ 7 solutions containing different concentrations of α-CD and β-CD. In the above CDs, the absorption maxima of MO and MR appeared at 463, 272 nm and 520, 274 respectively. A small but clearly observable effect appeared below a CD concentration of 0.01 M. In CD solutions, the absorbance slightly increased at the same wavelength. The inset Figures. 2 and 3 depict the changes in the absorbance and fluorescence intensity was observed as a function of the concentration of CD added. The above results were due to the transfer of guest from more protic environments (bulk aqueous phases) to less protic CD nano cavity environments [15-17].

Figures. 2 and 3 depict the emission spectra for MO and MR (excited at 460 nm and 510 nm) with varying concentration of α-CD and β-CD. In aqueous and CD solutions, MO and MR gave one emission maximum. Interestingly, in MO and MR, a similar absorption and emission spectral maxima were observed as in the CD solutions indicating that the both dyes form a similar type of inclusion complexes. The presence

of isosbestic point in the absorption spectra of the above CDs suggested that MO and MR form 1:1 inclusion complex with the CDs. The K value which is the association constant for the formation of 1:1 inclusion complexes can be evaluated from double reciprocal plot concerning the absorption and fluorescence intensity change [18]:

$$/I_f - I_0 = 1/\alpha + 1/\alpha K [CD]_0 \quad (4)$$

where I_f, I_0, α are the fluorescence intensities in the presence and absence of CD and the proportionality constant respectively. Figure. 3.3 illustrates the double reciprocal plot for the drugs containing the CDs. The straight line in the Figure. 3.3 confirms the 1:1 stochiometry of the CD –dyes inclusion complex. From the plot, the K value is estimated.

The stoichiometry of the inclusion complexes of the dyes with the CDs are studied by using Jobs method [19]. A plot of $(A-A_o)/A_o$ (or) $(I-I_o)/I_o$ versus [CD]/([CD]+[dyes]) gave a very good linearity as shown in Figure. 3.3. This analysis showed that azo dyes molecule form 1:1 inclusion complex with CD. Further the Benesi-Hildebrand plot [20] for 1:2 inclusion complex (dyes: CD) showed upward curve which confirmed that the 1:2 complex was not formed (Figures not shown).

The similar slopes in Figures. 4 for all the inclusion complexes indicate that the interactions of hydrogen atoms are approximately same in both the ground and excited states.

The hydrophobic contact with the guest is somewhat weak, since the polar substituents are far from the internal surface of the CD nano cavity and the SO_3Na group encapsulated in the interior part of the CD cavity. Further, the increased absorbance and emission intensities along with CD concentrations revealed that aromatic ring was encapsulated in the non-polar CD nano cavity. The small formation constant implies that the guest was not tightly embedded in the CD cavity.

Since the CD nano cavities restrict the free rotation of the guest, the emission intensity and quantum yield were increased in all the CD solutions. The presence of broad emission in CD aqueous solution suggested that viscosity plays a major role in the inclusion process. The increase in full width at half maximum (FWHM) of emission spectra with increasing CD concentration further supported the above prediction. Further it is well known that, the cavity size of the CD is also responsible for the different association constants.

The small association constant implied that the guest was not tightly encapsulated in the CD cavity. In other words, the SO_3Na is more deeply entrapped in the non-polar CD cavity than the CH_3-N-CH_3 groups. The gradual enhancement of emission with increasing CD concentration is consistent with this speculation.

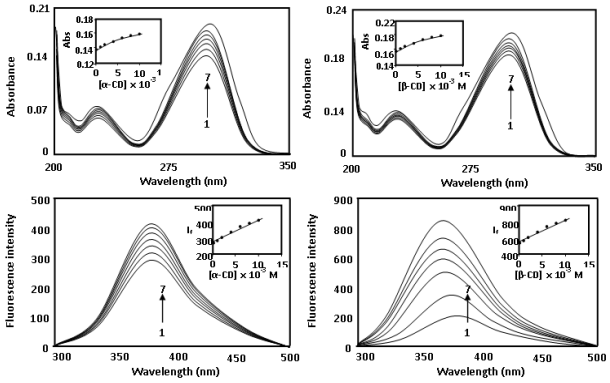

Figure – 2: Absorbance and fluorescence spectra of MO in different CD (-α & -β) concentrations (M): 1) 0, 2) 0.001, 3) 0.002, 4) 0.004, 5) 0.006, 6) 0.008, 7) 0.01; Inset figure: abs vs [CD] × 10^{-3} M.

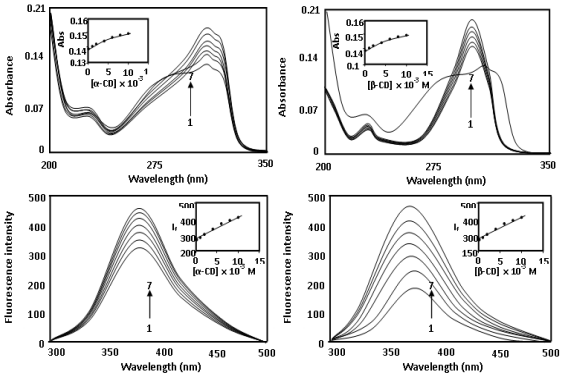

Figure – 3: Absorbance and fluorescence spectra of MR in different CD (-α & -β) concentrations (M): 1) 0, 2) 0.001, 3) 0.002, 4) 0.004, 5) 0.006, 6) 0.008, 7) 0.01; Inset figure: abs vs [CD] × 10^{-3} M.

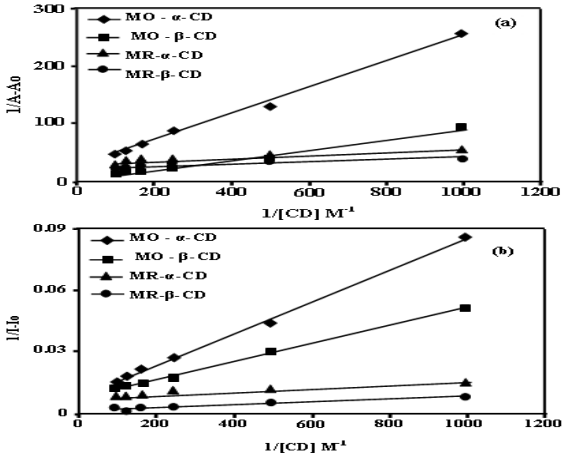

Figure – 4: Benesi-Hildebrand plot for the complexation MO and MR with CDs. Plot of $1/\Delta A$ *Vs* 1/[CDs] and Plot of $1/ (I - I_0)$ *Vs* 1/ [CDs].

Thus, the enhancement of the emission in CD indicated that the energy barrier is not affected by the entrapment of the guest in the non-polar CD cavity. Further, the presence of SO_3Na does not significantly change the inclusion process. The above findings confirmed that the hydroxyl group is present in the wider rim part and SO_3Na group is entrapped in the interior part of the CD cavity. As discussed above the orientation of the guest is same in the CD inclusion complexes.

3.2. Excited singlet state life time

The formation of inclusion complex was also studied by the fluorescence decay curves obtained for CD. Single exponential decay was observed for MO and MR in aqueous solution (1.93 ns). By the addition of the CDs, single exponential curve becomes biexponential. This showed MO and MR encapsulated in the CD cavity. The life time of azo dyes increased by the following order: water < α-CD < β-CD. The above order indicated that the tendency of complexation ability of CD, in other words β-CD has given the privileged encapsulation. The amplitude of the complexed component also increased due to increase in the complex formation and that of the decreased free species. The increase in the value of τ_1 and τ_2 with increase in the CD concentration is due to the encapsulation of MO and MR in the CD cavity. The τ_1 and τ_2 values depend on the type of CD and the nature of the process with regard to short-lived species. The decay of the MO and MR is dependent of the CD. This may be due to the vibrational restriction of MO and MR in the excited state. With native CD, the lifetimes do not change considerably, but the lifetime is high in CDs.

The increase in the lifetime of the MO and MR with longer lifetime in CDs is explained by confinement effect experienced by the fluorophore within the cavities of these CDs. The decrease in the amplitude of the MO and MR signifies a weaker interaction with the CD. The greater degree of encapsulation in β-CD than in α-CD is provides a stronger interaction than native CDs. The fact that, the fluorescence decays become single-exponential low in native CDs. This has been explained in the light of the difference in the orientation of the MO and MR molecule in the complexes with the CDs, which results from a difference in the size of their cavities. The longer lifetime is ascribed to a deep encapsulation (inside the cavity) and short life time is due to a loosely associated form. The difference in the extents of enhancement of fluorescence quantum yield of MO and MR induced by the two CDs may be explained similarly. A deep encapsulation with the smaller CD may be expected, compared to the loose complex with native CDs. This may be expected to cause a greater enhancement of fluorescence in the former than in the latter.

3.3. MOLECULAR MODELING STUDIES

3.3.1. HOMO - LUMO Parameters

The energy, HOMO, LUMO, thermodynamic parameters (enthalpy, entropy, free energy), chemical potential (μ), stability (S), dipole moment (D), hardness (η), electrophilicity (ω), zero point vibrational energy and Mulliken charge of the guest [methyl orange (MO) and methyl red (MR) (**Figure 1**)], host (α-CD and β-CD) and inclusion complexes are summarized in **Table 1**. From **Figure 5 and 6**, it can be seen that the guest molecules formed stable inclusion complexes with CD molecules. Interestingly, it was observed that the structure of the above two dyes:CD inclusion complexes were very similar to each other. The structural similarity could be a factor that made the complexation energies of β-CD with the guest molecules same.

From **Table 1**, it was found that, (i) chemical potential and HOMO of MO are more negative whereas electrophilicity of MO was more positive than that of MR, (ii) dipole and hardness of MO is larger than that of MR, (iii) HOMO-LUMO gap for MO was higher than MR, (iv) chemical potential of MO:β-CD was less negative than that of MR inclusion complexes, (v) dipole and the HOMO-LUMO gap for MO inclusion complex were larger than the MR complexes, (vi) no marginal difference was observed in the stability of the two dyes and their complexes, (vii) high negative ΔE was noticed in the β-CD inclusion complexes, (viii) electronic energy, Gibbs free energy, enthalpy and entropy of dyes were more negative than MR and (ix) entropy values for both the dyes and the inclusion complexes were negative.

The (E_{HOMO}-E_{LUMO}) gap is an important scale of stability [21] and compounds with large (E_{HOMO}-E_{LUMO}) values tend to have higher stability. So, we investigated the electronic structure of the complexes in with these considerations using PM3 method. The HOMO–LUMO energy gap of these dyes and their inclusion complexes were calculated using PM3 and are shown in **Table 1 and Figure 7,** which revealed that the energy gap reflected the chemical activity of the molecules. The LUMO as an electron acceptor represents the ability to obtain an electron and HOMO represents the ability to donate electron.

Moreover, a lower HOMO–LUMO energy gap explained the eventual stability of the complex i.e., isolated molecule had lower stability than complex molecule. The E_{HOMO}-E_{LUMO} gap (**Table 1**) confirmed that the stability of the dye - β-CD inclusion complexes were more stable. **Figure.** 7

indicated that the HOMO-LUMO energy gaps of all these complexes were significantly varied. The energy gap between HOMO and LUMO of each complex suggested a significant change in the electronic spectrum of the guest molecules driving molecular recognition and binding. This suggested the stability of these inclusion complexes were same.

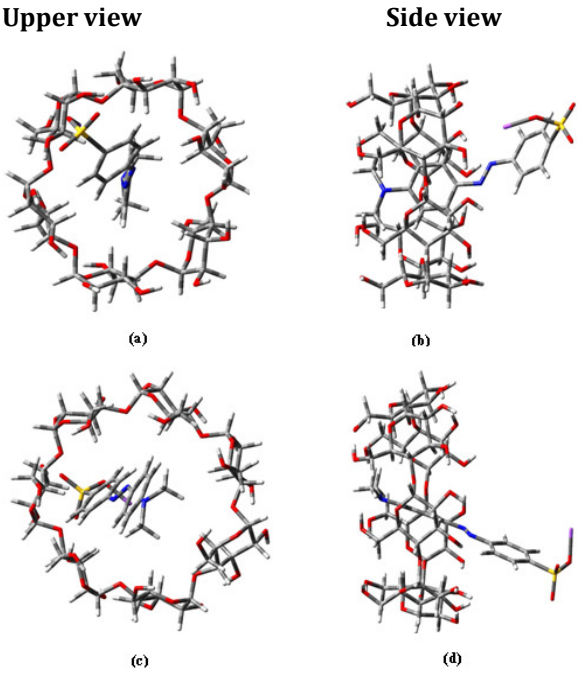

Figure – 5: Upper and side views of low energy structures calculated for the complexes between α-CD and β-CD with methyl orange.

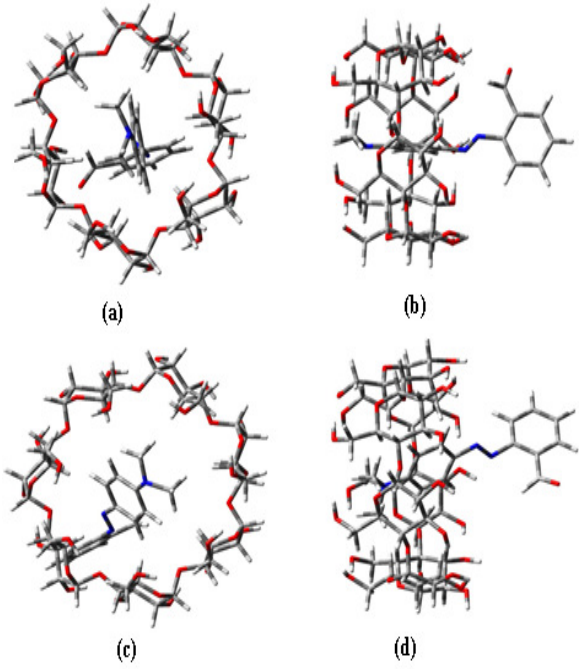

Figure – 6: Upper and side views of low energy structures calculated for the complexes between α-CD and β-CD with methyl red.

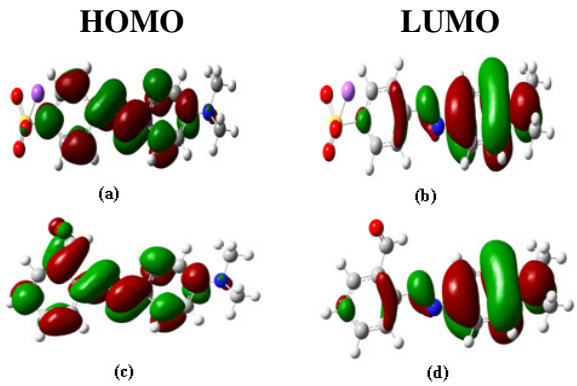

Figure – 7: The HOMO, LUMO energy structure of Methyl orange and methyl red.

The HOMO of these dyes was slightly varied (**Table 1** and **Figure. 7**) indicating inclusion complexation processes differ from each other. The inclusion complexes dipoles were higher than isolated dyes, where as lower than β-CD. This is because the polarity of the β-CD cavity decreased after the dye entered the cavity. The above quantum mechanical computations demonstrated a strong relationship with the complexation behavior. One can therefore conclude the dipole moment values having a strong a correlation with the complexation behavior. However, it is not straight forward why the complexation of β-CD with dye is more favorable than others if the dipole-dipole interaction and hydrophobic interaction are the only driving forces in β-CD complexation.

Though the results are not readily understandable, the Morokuma theory of energy decomposition analysis [22] can offer a reasonable explanation. According to the theory, when a supermolecule was formed, electrons will lose their identity as belonging to one or other component molecule. Four types of interactions should be considered in the formation of a supermolecule: (a) electrostatic interaction, which is favored by large permanent charges and dipoles, (b) polarization interaction, which is favored by large volume and polarizability of the molecules, (c) exchange energy, or Pauli repulsion and (d) charge-transfer interaction, which is resulted from the mixing of the filled orbital of one component molecule with the vacant orbital of the other.

The charge-transfer interaction is always attractive and the most important terms in this interaction are contributed from the charge-transfer between the HOMO of one component and the LUMO of the other. The first three interactions constitute the canonical driving forces in CD chemistry, i.e., dipole–dipole interaction, dipole-induced dipole interaction and steric effect.

Table - 1: Binding energies and HOMO-LUMO calculations for the inclusion complexes using PM3 method

Properties	MO	MR	α-CD	β-CD	MO :α-CD	MR :β-CD
E_{HOMO} (eV)	-8.99	-9.19	-10.37	-10.35	-9.05	-9.01
E_{LUMO} (eV)	-0.91	-0.92	1.26	1.23	-1.12	-0.89
$E_{HOMO} - E_{LUMO}$ (eV)	-8.08	-8.29	-11.63	-11.58	-8.12	-8.05
μ	-4.65	-5.14	-4.56	-4.56	-4.86	-4.99
η	4.24	4.21	5.81	5.79	4.27	4.14
ω	3.18	2.19	1.78	1.79	3.11	2.05
S	0.29	0.23	0.17	0.17	0.24	0.25
Dipole (D)	6.19	5.22	11.34	12.29	6.81	5.94
E Kcal $mole^{-1}$	-23.95	-11.87	-1247.62	-1457.63	-1254.05	-1506.19
ΔE Kcal $mole^{-1}$					19.63	-22.50
G Kcal $mole^{-1}$	-126.05	-96.26	-676.37	-789.52	-533.57	-701.13
ΔG Kcal $mole^{-1}$					56.32	1.92
H Kcal $mole^{-1}$	-167.82	-119.93	-570.84	-667.55	-415.33	-528.91
ΔH Kcal $mole^{-1}$					36.60	-7.54
S Kcal/mol-Kelvin	-0.1801	-0.1264	0.353	0.409	0.430	0.476
ΔS Kcal/mol-Kelvin					-0.025	-0.075
Zero point Vibrational energy	156.18	138.91	635.09	740.56	795.24	887.13
Mulliken properties	0.00	0.00	0.00	0.00	0.00	0.00

However, they cannot explain the unexpected theoretical and experimental observations. The higher the HOMO of the guest molecule, the stronger is the charge-transfer interaction in the complexation. Here, the quantum mechanical studies indicate that no charge-transfer interactions are present in the four drugs with β-CD. Mulliken charge values for all the four complexes were zero, confirmed no charge transfer interactions are present in the β-CD complexation. Interestingly, β-CD is ready to act as Lewis acid accepting electrons, but the sulphonamide guests do not act as Lewis bases donating electrons. Thus, no charge transfer interactions are present between the HOMO of the drug compounds and the LUMO of β-CD.

3.3.2. Thermodynamics Parameters

To investigate the thermodynamics of the inclusion process, the binding energies (ΔE), Gibbs energy changes (ΔG), enthalpy changes (ΔH) and entropy changes (ΔS) for the most stable inclusion complexes (both Head-up and Head-down configurations) were calculated and summarized in **Table 1**. The complexation energy allowed us to evaluate the inclusion process and to find the most stable inclusion complex between the complexes studied. It was evaluated as

$$\Delta E_{complexation} = E_{complex} - (E_{\beta\text{-}CD} + E_{drug}) \quad (5)$$

where $E_{complex}$, $E_{\beta\text{-}CD}$ and E_{drug} represent the total energy of the complex, the free optimized β-CD and the free optimized drugs respectively. All the complexation energies were more negative than isolated drugs and β-CD. The lowest values for complexation energy correspond to the most stable complex. The higher binding energy (ΔE) of the complexes suggested that stability of complex is more compared to isolated molecule.

The energy involved in hydrogen bond interaction is also responsible for the higher/lower binding energy compared to those of the substituted/unsubstituted molecules. From **Table 1** and **Figures 5 and 6** marginal variations were noticed in ΔE for MO:β-CD inclusion complex. This confirmed that hydrogen bonding interaction played significant roles in the complexation process. Hence 'ΔE' value the MO inclusion complex is higher than that of other drug complexes. The 'ΔE' values are a reasonable measure of hydrogen bonding and the change in hydrogen bonding of the dye are caused only by the hydrogen ion concentrations.

The free energy, enthalpy and entropy for the inclusion complexes were more negative than that of isolated drug and β-CD. The negative free energy change (ΔG) of the inclusion complexes

suggest that the inclusion proceeded spontaneously at 303 K. The high negative ΔG value for MO:β-CD inclusion complex indicated that this inclusion process is more spontaneous than other complexes. The difference in ΔE and ΔG can be explained by the solvent effect. The experiments are conducted in aqueous medium and the computational work was done at vacuum phase. We were unable to do the computational work at the aqueous medium due to system limitation.

Due to the large molecular size of β-CD, calculations for these systems could not be performed for aqueous solutions and excited state. However, it was observed that the solvent effect on the host-guest interactions easily changed the inclusion reaction from a non-spontaneous process in the gas phase to a spontaneous one in the aqueous phase. The host-guest interaction causes an enthalpy-entropy compensating process in the gas phase whereas the same interaction caused an enthalpy-entropy co-driven process in aqueous solution, because inclusion complexation releases a number of water molecules from the cavity of β-CD.

Recently, some authors who encountered this discrepancy used the experimental values to modify their calculations. For example in the case of the complexes of both *cis* and *trans* isomers of Brooker's mercyanine inserted within β-CD cavity, the author's preliminary calculations of ΔG values predicted the complex would not form spontaneously and the magnitude and the sign of ΔS and ΔG values varied from the experiment values [23]. They argued that, experimentally the entropy of complexation depends on both the insertion of the dye molecule and the concurrent displacement of water molecules that are trapped with in the β-CD cavity. The water molecule should be included in the calculations and then they found the thermodynamic values closer to the experimental results and the sign matched the reported values in all cases.

Further S.K. Xing et al [20] proposed a model to calculate ΔS for the inclusion complex in aqueous solution with the assumptions that the effect of water molecules on the entropy changes of the 2-hydroxy-5-methoxyacetophenone:β-CD system is mainly determined by the water molecules in the β-CD cavity and the effect of the H_2O molecules out of the cavity is less important and thus can be negligible.

The very small negative ΔH values indicated that the inclusion formations of drugs with β-CD are an exothermic and enthalpy-driven ΔH > ΔS. It should be noted that ΔH and ΔS values contain contributions from (i) release of cavity found water, (ii) partial destruction of hydration shells of the reagents, (iii) non covalent interactions (van der Waals, hydrophobic and electrostatic interactions as well as hydrogen bonding and (iv) hydration of the complexes. All these process should be taken into account while discussing thermodynamic parameters of complex formation.

The small negative ΔS is a confirmation of restriction of freedom of the molecule and formation of less compact structures. As it is evident from **Table 1**, hydroxyl groups reduce binding affinity of β-CD to dyess, making the complexation process more enthalpy and less entropy favourable. It is assumed that the β-CD cavity size and drugs substituents serve as a steric hindrance for the drug inclusion.

The small negative ΔS values were assumed to be due to enhancement of disorder in the system. Moreover hydrophobic interactions, which are long range interactions, can be important in the β-CD complex formation.

The inclusion complex structure in **Figures. 5 and 6** also suggested that benzene ring was partially inside the cavity and interacts with it through hydrophobic interactions. Further the small ΔH values can be explained by the prevalence of hydrophobic interactions. Comparison of ΔH and ΔS showed that enthalpy changes are higher and entropy changes are lower for the complexation. Therefore complexes of the drugs with β-CD are more enthalpy stabilized.

The optimized inclusion structure in **Figures. 5 and 6** showed, hydrogen bond is formed in CD inclusion complex. The intermolecular hydrogen bonds were formed between hydrogen atom of amino group of the dyes and oxygen atom of primary hydroxyl group of the β-CD with a $d_{H\cdots O}$ distance less than 3.00 Å. This justified the importance of both interaction between the drugs and β-CD necessary to ensure better inclusion of the guest to the host. The above values were supported by the fact that the flexibility of the host molecule may be one of the structural requirements for inclusion complexes formation. Though the above dyes had similar volumes, polarizability and hydrophobicity, β-CD complexation with MO was stronger than that with MR.

The bond distances, bond angles and the most interesting dihedral angles of the dyes before and after complexation in CD obtained from PM3 calculations for the most stable structure (**Figures. 5 and 6**) are presented in **Table 2** (not shown). It was evident that in β-CD the geometry of the dyes are slightly altered.

The alterations were significant in dihedral angles, which indicated that the dyes adopted a specific conformation to form a stable complex. The internal diameter of β-CD is approximately 6.5 Å and the height is 7.8 Å. Considering the shape and dimensions of β-CD, the both dyes cannot be completely embedded in the β-CD nano cavity. The vertical distance and length of the dyes are greater than the upper/lower rim of β-CD. Hence, the aromatic rings cannot be fully present inside of the β-CD nano cavity. Further, the optimized theoretical structure of drugs: β-CD inclusion complex by Gauss view method also confirmed the drugs are partially included in the β-CD nano cavity.

It is well known that the van der Waals forces including the dipole–induced dipole interactions are proportional to the distance between guest, the wall of the β-CD cavity and to the polarizabilities of the two components. The interaction of the phenyl ring with β-CD would play an important role because the phenyl moiety may achieve a maximum contact area with the internal surface of the cavity of the CD.

The above results suggested the inclusion of the dye molecules with CD nano cavity is affected by hydrophobic and electronic interactions. Since CD has a permanent dipole the primary hydroxyl end is positive and the secondary hydroxyl end is negative in the glucose units of CD. The stability of binding by hydrophobic interaction is partly the result of van der Waals force but is mainly due to the effects of entropy produced on the water molecules**.** In the aqueous solution, a hydrophobic guest compound is restricted by the water shell formed by the hydrogen bonding network. It has a strong tendency to break down the water cluster and penetrate the non-polar cavity of the CD. This process is exothermic due to entropic gain. The energy for the inclusion of CD with guest compounds were observed to be proportional to the substituent hydrophobic constant of the guest.

4. CONCLUSION

The study of inclusion complexation of methyl orange and methyl red dyes with α-CD and β-CD, performed by UV-Visible, fluorescence, time resolved fluorescence, and molecular modeling techniques. Increases in fluorescence lifetime in CDs solution suggest that both dyes form stable inclusion complexes with CD molecules. The UV–visible and fluorescence results confirmed the formation of the inclusion complex and indicated an unconventional complex stoichiometry of 1:1 (dye–CD) in lower CD concentrations and 1:2 (dye–CD) with higher CD concentrations. From the computational study, we find that negative complexation energy, Gibbs energy and enthalpy changes for the inclusion complexes indicate that the formation of these complexes is spontaneous, exothermic and hydrogen bonding interactions play a major role in the inclusion process.

Acknowledgement

The authors thank Dr. N. Rajendiran, Associate Professor, department of chemistry, Annamalai University, for his help in the UV and fluorescence measurements.

5. REFERENCES

1. Szejtli J. Introduction and general overview of cyclodextrin chemistry, Chem. Rev. 1998, 98: 1743– 1753. PMID: 11848947
2. Carrier RL, Miller LA, Ahmed I. The utility of cyclodextrins for enhancing oral bioavailability. J Control Release, 2007, 123 (2), 78–99. doi: 10.1016/j.jconrel.2007.07.018 PMID: 17888540
3. Yuan C, Jin Y, Xu XM. Inclusion complex of astaxanthin with hydroxypropyl-β-cyclodextrin: UV, FTIR, 1 H NMR and molecular modeling studies increase the solubility. Carbohyd Polym, 2012, 89: 492–496
4. Jin X, Zhang ZH, Sun E, Li SL, Jia XB. Statistically designed enzymatic hydrolys is of anicariin/β-cyclodextrin inclusion complex optimized for production of icaritin. Acta Pharmaceutica Sinica B, 2012, 2 (1):83–89.
5. Hwang YY, Shin DC, Nam YS, Cho BK. Characterization, stability, and pharmacokinetics of sibutramine/β-cyclodextrin inclusion complex. Journal of Industrial and Engineering Chemistry, 2012, 18: 1412–1417.
6. Wang CQ, Wang RB, Zhao XX, Liu ZH, Wang DH. Preparation of β-cyclodextrin inclusion compound of volatile oil of Chrysanthemiflos and characterization analysis. J Gansu college of TCM, 2013, 30(6):29– 32.
7. Miao EZ, Zhang CL. Orthogonal Experiment on β-Cyclodextrin Inclusion of Volatile Oil from Chinses Angelica and Rhizome of Chuanxiong. J Liaoning University of TCM, 2013, 15(5):67–68.
8. Chen X, Xie HY. Technology research on β-cyclodextrin and camphor inclusion. Zhongguo Zhongyi Keji. 2013, 20(5):499–500.
9. Guo T, Wang ZY, Song HT, He J, Yan M. Preparation and Identification of the Inclusion Complex of Garlic Oil with 2-Hydropropyl β–

Cyclodextrin. Pharm J Chin PLA, 2006, 22(2): 91–94.

10. 9. Burke, N. S.; Crawford, D. L. Use of azo dye ligand chromatography for the partial purification of a novel extracellular peroxidase from Streptomyces viridosporus T7A. Appl. Microbiol. Biotechnol. 1998, 49, 523–530.
11. 10. Vicente, S.; Manisso, N.; Queiroz, Z. F.; Zagatto, E. A. G. Spectro-photometric flow-injection determination of nickel in biological materials. Talanta. 2002, 57, 475-480.
12. 11. Khedr, A. M.; Gaber, M.; Issa, R. M.; Erten, H. Synthesis and spectral studies of 5-[3-(1,2,4-triazolyl-azo]-2,4-dihydroxybenzaldehyde (TA) and its Schiff bases with 1,3-diaminopropane (TAAP) and 1,6-diaminohexane (TAAH). Their analytical application for spectrophotometric microdetermination of cobalt(II). Application in some radiochemical studies. Dyes and Pigments. 2005, 2, 117-126
13. T. Steiner G.J. Koellner, Am. Chem. Soc. 116 (1994) 5122-5128.
14. (a) L. Liu, Q.X. Guo, J. Incl. Phenom. Macrocycl. Chem. 50 (2004) 95-103. (b) A.A. Rafati, S. M. Hashemianzadeh, Z.B. Nojini, M.A. Safarpour, J. Mol. Liq. 135 (2007) 153-157.
15. Bardi L, Mattei A, Steffan S, Marzona M. Hydrocarbon degradation by a soil microbial population with beta-cyclodextrin as surfactant to enhance bioavailability. Enzyme Microb Technol 2000;27:709–713.
16. K.B. Lipkowitz, Applications of Computational Chemistry to the Study of Cyclodextrins, Chem. Rev. 98 (1998) 1829-1874.
17. Lei Liu, Ke-Sheng Song, Xiao-Song Li, Qing-Xiang Guo, Charge transfer interaction: A driving force for cyclodextrin inclusion complexation, J. Inclu. Pheno. Macrocyc. Chem. 40 (2001) 35-39.
18. D. Bogdan, C. Morari, Electronic structure and driving forces in β-cyclodextrin:
19. Diclofenac inclusion complexes, Physics Letters A 366 (2007) 454-459.
20. S.K. Xing, C. Zhang, H.Q. Ai, Q. Zhao, Q. Zhang, D.Z. Sun, Theoretical study of the interactions of β-cyclodextrin with 2′-hydroxyl-5′-methoxyacetophone and two of its isomers, J. Molecular Liquids, 146 (2009) 15-22.
21. M. Karelson, V.S. Lobanov, R. Katrizky, Quantum-Chemical Descriptors in QSAR/QSPR Studies, Chem. Rev. 96 (1996) 1027-1044.
22. K. Morokuma, Why do molecules interact? The origin of electron donor-acceptor complexes, hydrogen bonding and proton affinity, Acc. Chem. Res. 10 (1977) 294-300.
23. H. Hamdi, R. Abderrahim, F. Meganem, Spectroscopic studies of inclusion complex of β-cyclodextrin and benzidine diammonium dipicrate, Spectrochim. Acta 75A (2010) 32-36.